Magnetoacoustic Measurements of the Fermi Surface of Aluminum*†

G. N. KAMM AND H. V. BOHM
Department of Physics, Wayne State University, Detroit, Michigan
(Received 14 February 1963)

The magnetoacoustic pulse-echo method has been applied to a study of the Fermi surface of aluminum, using 350-Mc/sec longitudinal sound waves. Single-crystal samples were studied with the sound propagation along the three principal crystallographic directions. A considerable variety of oscillation periods have been observed. The experimental results are presented and discussed with reference to several models. A redetermination of the low-temperature adiabatic elastic moduli of aluminum from ultrasonic pulse-echo velocity measurements has yielded values which, though differing from earlier published values, give a much better correlation of our data with the Fermi surface models. Some rough estimates are made of the electron relaxation times for the crystals used.

INTRODUCTION

THE Fermi surface of aluminum has been the subject of a number of investigations. Information about the Fermi surface has been obtained using several experimental methods: specific-heat measurements,[1] de Haas–van Alphen measurements,[2–4] anomalous skin effect experiments,[5] magnetoresistance studies,[6,7] cyclotron resonance studies,[8–12] and magnetoacoustic experiments.[13–17] Band-structure calculations for aluminum have been made by Heine,[18] Harrison,[19–21] and Segall.[22]

The results of the band-theory calculations and the experimental measurements are consistent with a Fermi surface volume of about three electrons per atom, a surface that overlaps the boundaries of the first Brillouin zone on each face and that, at least in regions removed from the zone boundaries, nearly matches the free-electron model. In the vicinity of the zone boundaries, the details of the surface have been less accurately determined by theory and experiments. The present studies were undertaken in the hope that with improved resolution and accuracy, magnetoacoustic measurements might yield some information on possible multiply connected regions and other details of the surfaces in the second and third zones, as well as allowing a comparison with various theoretical models and experimental results obtained by other techniques.

On the basis of low-field de Haas–van Alphen measurements by Gunnersen,[2] band calculations by Heine[18] led him to suggest a model for the Fermi surface having pockets of holes at the far corners of the first zone, a second zone structure interconnected in the corresponding regions, and a third zone consisting of isolated pieces. Harrison pointed out[19] that the same experimental data was consistent with a model having a closed second zone and interconnected arms in the third zone. The shape of such arms and the modifications of the second zone structure were then calculated by him on a 4-OPW (orthogonalized plane wave) model[20,21]; more recently, Segall[22] has extended and refined calculations of the band structure and Fermi surface. That the third zone conformation has the nature of elongated arms is demonstrated unambiguously by recent data of Gordon and Larson[4] who repeated and extended Gunnersen's de Haas–van Alphen work with higher resolution. It is also indicated by the cyclotron resonance data of Moore and Spong,[11] and shown more clearly in that of Galkin, Naberezhnykh, and Melnik.[12]

None of these data determine conclusively whether

* This research was supported by the U. S. Air Force through the Office of Scientific Research under Contract AF 49(638)-832, and later under Grant AFOSR 62-379.

† Based on a thesis (G. N. Kamm) submitted in partial fulfillment of the requirements for the degree of Doctor of Philosophy at Wayne State University, Detroit, Michigan.

[1] D. H. Howling, E. Mendoza, and J. E. Zimmerman, Proc. Roy. Soc. (London) **A299**, 86 (1955).

[2] E. M. Gunnerson, Phil. Trans. Roy. Soc. (London) **A249**, 229 (1957).

[3] M. G. Priestley, in *Proceedings of the Seventh International Conference on Low-Temperature Physics*, edited by G. M. Graham and A. C. Hollis Hallet (University of Toronto Press, Toronto, 1961), p. 230, and to be published.

[4] W. L. Gordon and K. Larson (private communication).

[5] E. Fawcett, in *The Fermi Surface*, edited by W. A. Harrison and M. B. Webb (John Wiley & Sons, Inc., New York, 1960), p. 197.

[6] R. G. Chambers, in *The Fermi Surface*, edited by W. A. Harrison and M. B. Webb (John Wiley & Sons, Inc., New York, 1960), p. 100.

[7] R. Balcombe, thesis, University of Cambridge (unpublished).

[8] D. N. Langenberg and T. W. Moore, Phys. Rev. Letters **3**, 137 (1959).

[9] E. Fawcett, Phys. Rev. Letters **3**, 139 (1959).

[10] E. Fawcett, in *The Fermi Surface*, edited by W. A. Harrison and M. B. Webb (John Wiley & Sons, Inc., New York, 1960), p. 166.

[11] T. W. Moore and F. W. Spong, Phys. Rev. **125**, 846 (1962); errata, **126**, 2261 (1962).

[12] A. A. Galkin, V. P. Naberezhnykh, and V. L. Melnik (to be published).

[13] B. W. Roberts, Phys. Rev. **119**, 1889 (1960).

[14] P. A. Bezugly, A. A. Galkin, A. I. Pushkin, and A. I. Khomchenko, Zh. Eksperim. i Teor. Fiz. **42**, 84 (1962) [translation: Soviet Phys.—JETP **15**, 60 (1962)].

[15] G. N. Kamm and H. V. Bohm, in Proceedings of the Eighth International Conference on Low-Temperature Physics, London, 1962 (to be published).

[16] P. A. Bezugly, A. A. Galkin, and A. I. Pushkin, in Proceedings of the Eighth International Conference on Low-Temperature Physics, London, 1962 (to be published).

[17] B. Jones, thesis, University of Bristol (unpublished).

[18] V. Heine, Proc. Roy. Soc. (London) **A240**, 340 ff (1957).

[19] W. A. Harrison, Phys. Rev. **116**, 555 (1959). The "far corners of the first zone" referred to above are the symmetry points marked *W* in Fig. 2 of this reference.

[20] W. A. Harrison, Phys. Rev. **118**, 1182 (1960).

[21] W. A. Harrison, Phys. Rev. **118**, 1190 (1960).

[22] B. Segall, Phys. Rev. **124**, 1797 (1961), and private communication.

or not these arms are interconnected. Magnetoresistance studies have also been inconclusive concerning the connectivity of the aluminum Fermi surface. A recent exhaustive study of the anisotropy of magnetoresistance in aluminum by Balcombe[7] still did not clearly show either the high-field saturation or square-law behavior usually associated with closed or open electron orbits, respectively.

THE MAGNETOACOUSTIC METHOD

Whereas cyclotron resonance experiments measure the orbits having extremal values of effective mass, the oscillations in the de Haas–van Alphen and magnetoacoustic methods measure purely geometrical properties of the Fermi surface, the former extremal areas and the latter extremal or caliper dimensions. It follows from the force equation for an electron in a magnetic field in the form $\hbar\dot{\mathbf{k}}=(e/c)\mathbf{v}\times\mathbf{H}$ that the Fermi surface orbit has the same form as the component of the real space orbit perpendicular to $\mathbf{H}$, but rotated by 90°. Magnetoacoustic oscillations arise from the strong interaction occurring when a portion of the electron's path lies in the plane of the sound wave. The integral of the force equation between two such regions gives the Fermi surface dimension Δk measured perpendicular to the constant magnetic field $\mathbf{H}$ and to the sound-wave propagation vector $\mathbf{q}$ as a function of the separation Δr of these regions measured in the direction of $\mathbf{q}$. The result is $\Delta k=[e/(c\hbar)]H\Delta r$. Maxima of attenuation are observed at integral values of n, and minima at half-integral values of n in the equation $\Delta r=(n+\gamma)\lambda$. The phase correction factor γ may take either positive or negative values. It is a function of n for small values of n, but very rapidly approaches a constant value as n increases, and, thus, the extremal points soon become linear in $1/H$. The radially measured Fermi surface dimension k, where $k=\Delta k/2$ is given as a function of the periodicity in $1/H$ by the relation

$$k=\frac{\lambda e}{2c\hbar}\frac{1}{\Delta(1/H)}.$$

In general, magnetoacoustic oscillations arise from extremal regions, i.e., regions where the orbit path lies in the plane of the sound wave and adjacent orbits yield the same value of k. Pippard[23,24] has pointed out, however, that a limited series of oscillations may well arise from regions which are not truly extremal if these regions exhibit a large coupling to the acoustic wave.

THE EXPERIMENTAL CONDITIONS

The aluminum samples used in the experiments were cut from single crystals grown from 99.9999% pure material.[25] For these samples at 350 Mc/sec and liquid-helium temperatures, the values of ql are much greater than unity, where $q=2\pi/\lambda$, and l is the mean free path of the electrons which is in our case impurity limited. The skin depth δ is much smaller than the wavelength λ.

Cyclotron resonances are not observed in the data because the value of $\omega_s\tau$ is always less than unity, ω_s being the sound angular frequency and τ the relaxation time; $\omega_s\tau$ is on the order of ql multiplied by the ratio (sound velocity/electron velocity). The velocity of the electrons is larger than the velocity of sound by a factor of about 300; thus the sound wave can be considered as essentially stationary in comparison to the orbital motion. Because of the high zero-field attenuation and the additional increase of attenuation with increasing field, it was necessary to limit the acoustic path in the metal to 1 or 2 mm; to separate the transmitted pulse from the main pulse a quartz crystal delay line was employed. The sample holder assembly and electronic equipment have been described elsewhere.[26] The samples were oriented within 0.5° of the {110}, {111}, and the {100} crystal planes, and finished flat and parallel within $\pm3\times10^{-5}$ in. over the area of the quartz transducers.

The magnetic field was measured with a rotating coil fluxmeter (Rawson type 720) with its coil about 1.5 in. from the sample but well within the uniform field region of the tapered 6-in. pole faces of the magnet (Varian type V4012-3B). The fluxmeter was calibrated and periodically checked against standard magnets of 1000 and 2644 Oe (Rawson type 721 and 721-H). The systematic error in the data from the magnetic-field measurements is estimated to be less than 0.5%. Measurements of frequency were made using a crystal-calibrated heterodyne frequency meter and have a maximum error of 0.1%. The 4.2°K value used for the lattice constant is $4.032_3\times10^{-8}$ cm, determined by making temperature corrections on Pearson's 77° data.[27,28] The values used for the longitudinal velocity of sound along the principal axes were determined in a subsidiary experiment discussed in a later section. Their error is 0.5% or less.

ANALYSIS OF THE EXPERIMENTAL DATA

The positions of the maxima and minima of attenuation were determined on the recorder chart record relative to the sloping background attenuation, which included oscillations of other periods, and plotted as a

[23] A. B. Pippard, in *The Fermi Surface*, edited by W. A. Harrison and M. B. Webb (John Wiley & Sons, Inc., New York, 1960), p. 230.

[24] A. B. Pippard, in *Low Temperature Physics*, edited by C. DeWitt, B. Dreyfus, and P. G. deGennes (Gordon and Breach, New York, 1962), p. 124.

[25] The crystals used for the ⟨110⟩ and ⟨111⟩ sound directions were grown by the Czochralski technique by Dr. James Kirn of Virginia Institute for Scientific Research. The crystal used for the ⟨100⟩ sound direction was kindly lent to us by Dr. Ben Roberts of the General Electric Research Laboratory and was one of the crystals used by him in his earlier experiments. (See reference 13.)

[26] G. N. Kamm and H. V. Bohm, Rev. Sci. Instr. **33**, 957 (1962).

[27] W. B. Pearson, in *Handbook of Lattice Spacings and Structures of Metals* (Pergamon Press Inc., New York, 1958).

[28] *Thermal Expansion of Technical Solids at Low Temperatures*, National Bureau of Standards Monograph No. 29 (U. S. Government Printing Office, Washington, D. C., 1961).

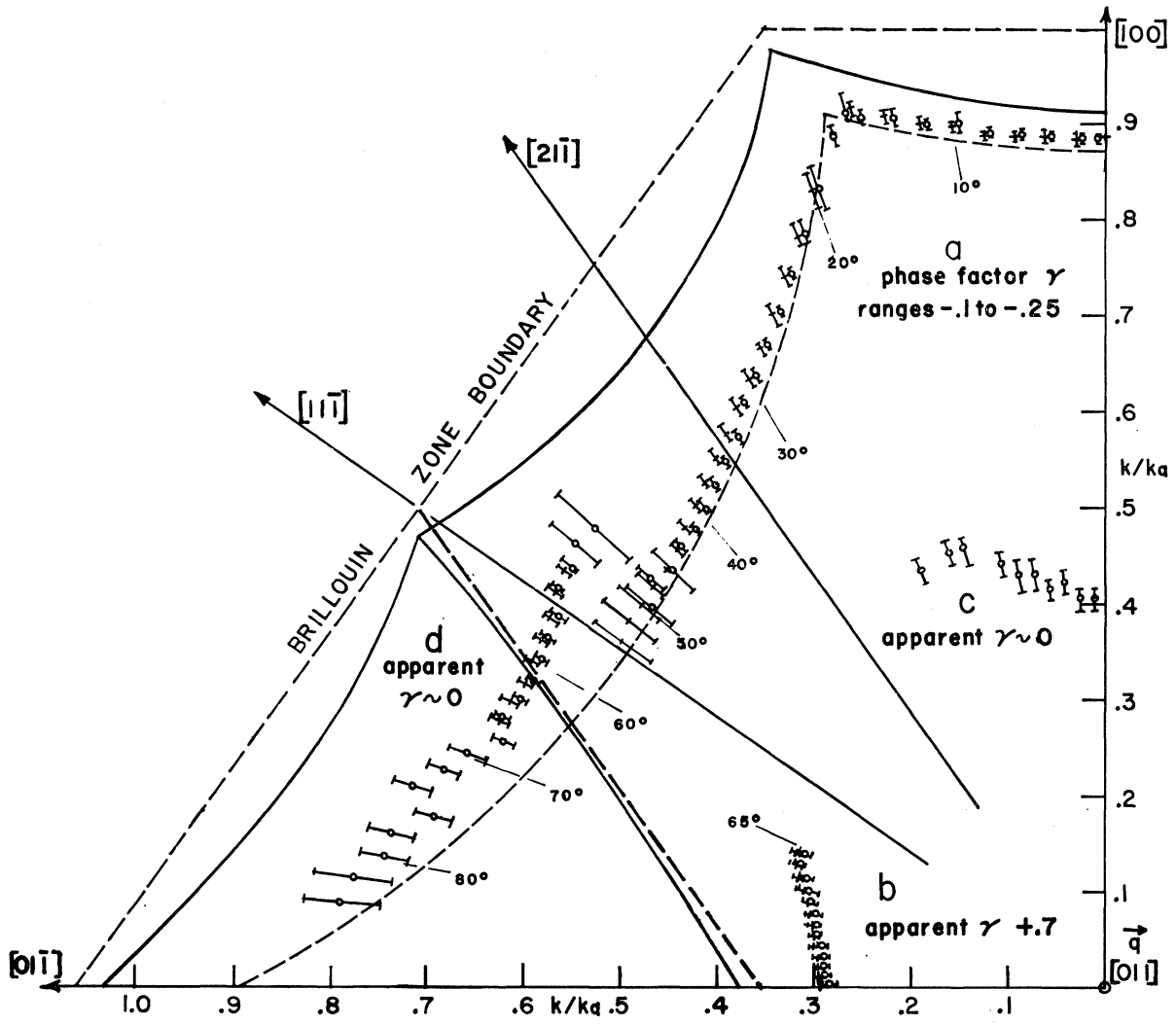

FIG. 1. {110} face data. Values of k/k_a are plotted from the origin. For comparison the free-electron surface is shown in outline (solid) and in its central section (dashed). The sound propagation vector **q** lies in the [011] direction, perpendicular to the page, and the magnetic field **H** lies in a (011) plane, i.e., the plane of the paper. Data points marked as circles and as crosses are from different runs and illustrate, as described in the text, the consistency of the data.

function of $1/H$. The slope of the best straight line through the extremal points, with less weight given to the lowest values of n, determines the value of k. The intersection with the $1/H=0$ axis of the extrapolated line, when taken together with an identification of the high field extrema, yields the limiting value of the phase factor γ; however, the high-field extrema could not always be identified because of the limited range of the magnetic field, and the mixing of the oscillations. The measured values of γ provide useful guides in identifying the oscillations, and suggest the local nature of the surfaces responsible for them. For example, from theoretical considerations,[13,24,29] one would expect limiting values of γ as follows: $\gamma=0$ for a rectangular form, $\gamma=+\frac{1}{4}$ for a circular cylinder, $\gamma=+\frac{3}{8}$ for a sphere, and negative values of γ for concave forms.

DESCRIPTION OF THE OSCILLATIONS

The oscillations for aluminum are never as prominent as the characteristic oscillations observed with the noble metals.[30–32] They occur against a background of attenuation which rises rapidly when the magnetic field strength exceeds a few hundred Oe. Figure 1 shows, in a reduced Brillouin zone, values of k determined from the magnetoacoustic oscillations on the {110} face. The

[29] M. H. Cohen, M. J. Harrison, and W. A. Harrison, Phys. Rev. **117**, 937 (1960).

[30] V. J. Easterling and H. V. Bohm, Phys. Rev. **125**, 812 (1962).
[31] H. V. Bohm and V. J. Easterling, Phys. Rev. **128**, 1021 (1962).
[32] R. W. Morse, in *The Fermi Surface*, edited by W. A. Harrison and M. B. Webb (John Wiley & Sons, Inc., New York, 1960), pp. 214 ff.

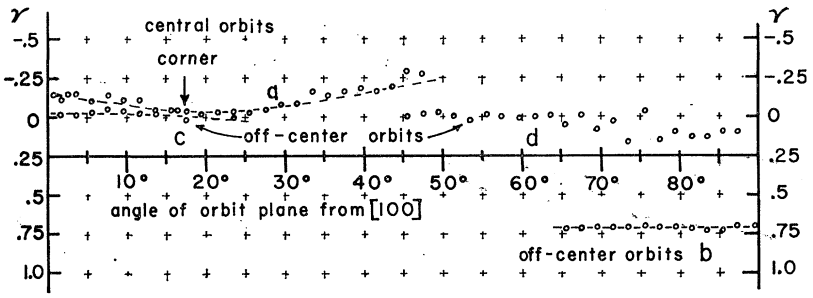

FIG. 2. Apparent phase factors γ for large n for the oscillation groups plotted in Fig. 1.

data points are plotted as dimensionless ratios k/k_a: Here k_a is the distance from the center of the zone to the zone boundary in the [100] direction and numerically equal to 2π divided by the lattice constant. The magnetic field is always perpendicular to the direction in which k/k_a is plotted.

At angles less than 45° from the [100] direction, the points of group a lie very close to the dashed line representing a central section of the free-electron model. In this group the strongest oscillations are in the [100] direction where 34 extrema are observed, the last (lowest H) at about 500 Oe. At angles between 16° and 20° the oscillations are weaker and only observed clearly at low fields. The phase factor in group a is negative and varies with angle as is shown in Fig. 2. Between 50° and 65° the oscillations of group d are prominent. They are characterized by larger value k/k_a and a phase factor nearly zero. Although this series continues to larger angles, beyond 65° it becomes secondary to group b which has strong oscillations with values of k/k_a about half the size of group d, and apparently a positive phase factor. Group b oscillations are strongest in the [01$\bar{1}$] direction where 16 extrema were observed, the last at fields of about 300 Oe.

An attempt was made to measure the secondary as well as the principal oscillations, but because the amplitudes are weaker and they are often observed only at high fields, the accuracy of the k values is less. A secondary set of oscillations marked as c in Fig. 1 is clearest in the [100] direction. This group can be distinguished near that direction by the alternation of amplitudes in the oscillations of the principal group a, and elsewhere by the occurrence of doubled peaks and beats within that group. The data plotted as circles and as crosses represent two runs made with different recorders and directions of magnetic field sweep (increasing or decreasing with time), and illustrate the consistency of the data.

The oscillations on the {111} face fall into two groups as shown in Fig. 3. Group b (having the smaller values of k) lies symmetrically about the ⟨110⟩ directions and in this direction 10 extrema were measurable. Although visible in the form of beats at angles up to ±18°, this group could be measured only up to ±12°. Group a, having a larger value of k, is visible at all angles. As many as 22 extrema could be measured, although only the first few were absolute maxima or minima; where mixed with the oscillations of group b, a could be distinguished only at higher magnetic fields, thus reducing the precision of the measurements. The symmetry of the Fermi surface requires that the pattern of magnetoacoustic oscillations exhibit reflection symmetry about the ⟨110⟩ and ⟨112⟩ directions. Data were taken over considerably more than 30° and this symmetry verified. In Fig. 3 the plotted points have been duplicated in accordance with this symmetry.

On the {100} face, the rapid rise of background attenuation as a function of magnetic field gives records on which many oscillations do not exhibit either absolute maxima nor minima, but only inflection points. In some cases the data at high fields was supplemented by data from earlier experiments at 230 Mc/sec where the attenuation is lower. Experimental results are given in Fig. 4. Well-defined oscillations labeled group b are observed, the values of k/k_a match that of Fig. 1 group b in the same direction. The oscillations are strong at most angles, though weaker in the neighborhood of 8° from the ⟨100⟩ directions. Moderately strong oscillations, observed at high fields near angles of 0° and 45°, are indicated by groups a and c, respectively. The phase of oscillations in groups a, b, and c could not be uniquely determined. The oscillation pattern on the {100} face must exhibit a reflection symmetry about the ⟨110⟩ and ⟨100⟩ directions. This was verified by taking data over a wide angular range, but in Fig. 4 and also in Fig. 5(b) the data points have been duplicated in accordance with this symmetry.

Oscillations at fields of 800 Oe and lower are observed on the {100} face at all angles. The values of k/k_a are plotted in Fig. 4 as group d and on a larger scale with the limits of error indicated in Fig. 5(b). They appear to be about equally strong except in the neighborhood of 10° and have an apparent phase $\gamma=+0.65$. A comparable group of oscillations occurs on the {110} face with similar periods and phase. Here, however, there were not enough extrema present to determine the periods accurately; therefore, the data are plotted on Fig. 5(a) as though all the oscillations had a phase $\gamma=+0.6$, approximately the same as those on the {100} face shown in Fig. 5(b). The amplitudes are strongest within ±4° of the [100] direction, and within ±8° of the [01$\bar{1}$] directions.

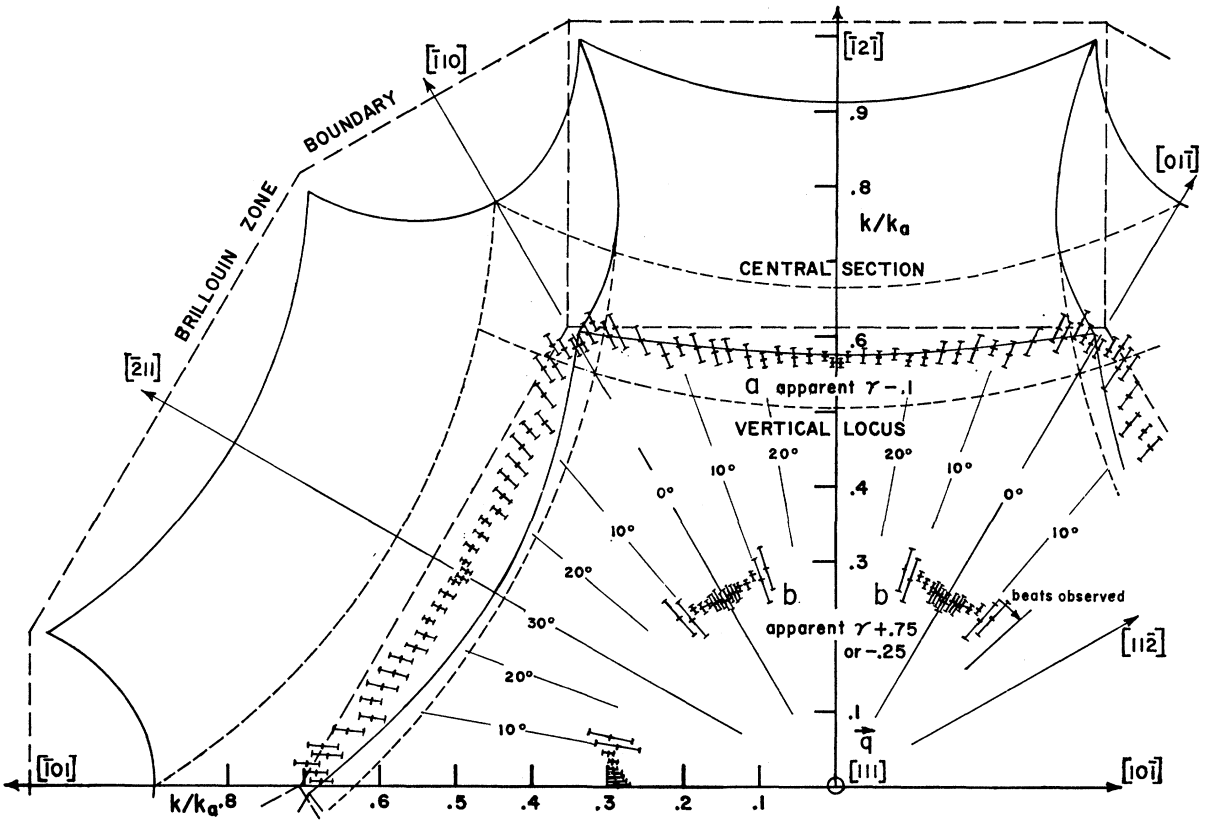

FIG. 3. {111} face data. Values of k/k_a are plotted from the origin. **q** is in the [111] direction, perpendicular to the page, and **H** is in the (111) plane. The central section of the Fermi surface and the locus of regions where the surface lies parallel to the direction of **q** are shown as dashed lines. The outline of the free-electron surface is shown as solid lines.

On the {110} face, at fields of 200 Oe and below are oscillations which represent the smallest observed values of k/k_a. It must be noted that since at most 4 extrema are observable, the accuracy of the measurements is poor. The data are plotted in Fig. 6 as though the oscillations all have a phase factor $\gamma=+0.06$. The points appear to form a pattern of three straight lines. Unresolved oscillations of comparable periods also exist on the other faces at low fields.

One expects the pattern of magnetoacoustic oscillations with increasing field to have a final minimum when the size of the orbit projection on a plane perpendicular to **H** becomes of the order of $\lambda/2$, after which the attenuation increases. In the case of aluminum, this final minimum for orbits of the smallest dimensions occurs at fields as low as 200 Oe. Thus, a monotonic increase in attenuation at higher fields associated with these orbits appears to be the background against which all of the other oscillations are observed.

The Fermi surface dimensions given in Table I are obtained from smooth curves drawn through the measured values. The limits of error given represent the total estimated error. The limits of error noted on Figs. 1, 3, 4, 5, and 6 are obtained from the maximum differences in the slopes of straight lines which can be drawn through the data points, but do not take into account the possible systematic errors arising from magnetic-field calibration, sound-frequency measurement, and the velocity of sound. The sum of the systematic errors adds an estimated 1% to the limits shown in these plots.

INTERPRETATION OF THE DATA

Some of the oscillations have a direct and obvious interpretation, but the interpretation of others presents some problems. Those data points on the {110} face, Fig. 1 group *a*, which lie close to the dashed line of the central section are interpreted naturally as arising from extremal regions and central orbits on the second zone surface. The negative values of γ also suggest such concave regions. Because of the relatively large experimental errors near the corner, the data could fit either a free-electron model or the calculated surface of Segall.[22] The sudden break near 50° to a larger value of k and a different phase can be explained if the group *d* is interpreted as due to off-center orbits for which one extreme is the rounded knife-edge in the $[0\bar{1}1]$ direction, and the other a broad concave spherical portion of the second zone surface. The opposite curvatures of such regions could be the explanation of the zero value of γ observed. In Table I, the measured dimensions are seen

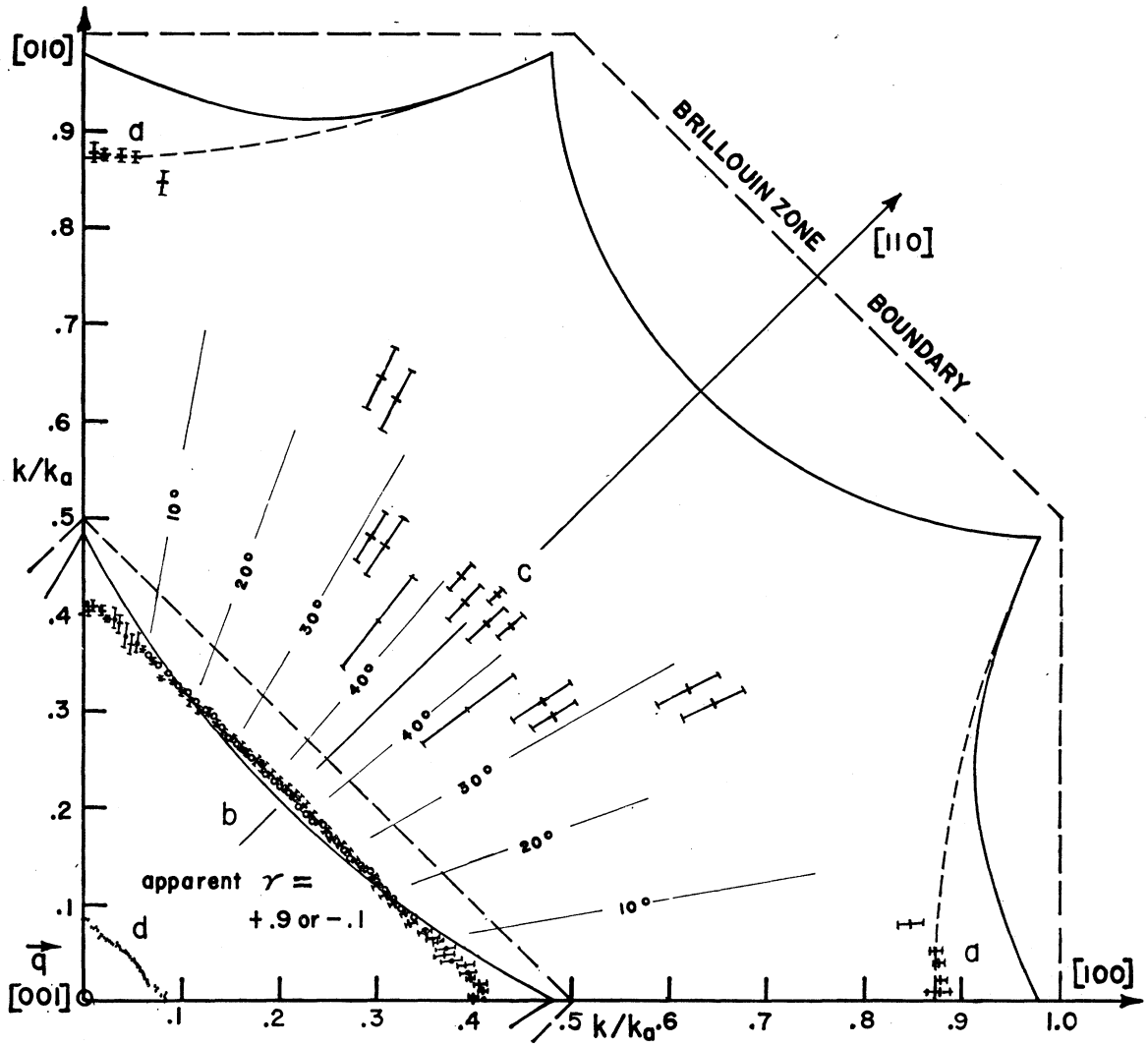

FIG. 4. {100} face data. Values of k/k_a are plotted from the origin. **q** is in the [001] direction, perpendicular to the plane of the page, and **H** is in the (001) plane. The free-electron surface is shown in outline (solid) and in its central section (dashed). Data points marked as circles and as crosses illustrate the consistency of the data.

to fit this interpretation quite well for the model of Segall.

The dimension and angular range of the strong oscillations of Fig. 1 group *b*, which are observed without discontinuity over angles ±35° from the [01$\bar{1}$] direction, lead us to believe that they arise from off-center 4-sided orbits on the second zone surface which pass around a "block-shaped" region. The measured dimension matches that expected from one edge to the broad concave region on the opposite side. It should be noted that on neither the free-electron model nor that of Segall are such regions strictly extremal. The edges mark reflecting planes of the crystal lattice in the extended zone and thus may be regions where the coupling is locally strong. This group, therefore, may be an example of oscillations from nonextremal regions, of the kind suggested by Pippard.[23,24] Within an angle of ±3° from the [01$\bar{1}$] direction the measured dimension also fits that of orbits which pass around the inside of the square arms in the third zone on the model of Segall.

No precise identification is offered for the rather weak series of oscillations of Fig. 1 group *c*. However, it may be noted that the dimension in the [100] direction matches that on the {100} face, Fig. 4 group *b*, in the same direction, leading us to speculate that the two oscillation groups may be associated with the same feature of the Fermi surface, but tilted by 45° from each other.

The edge regions which gave the strong oscillations of Fig. 1 group *b* are seen also on the other faces. The oscillations of Fig. 3 group *b* for the {111} face and of

Fig. 4 group *b* for the {100} face are very similar to those of Fig. 1 in period, amplitude, number of oscillations, and perhaps also in phase; although the magnetic-field direction is different for the three faces and the orbit shapes differ widely. The angular ranges of these oscillations on the {111} and {100} faces are consistent with the interpretation that the oscillations arise from edges of the "block-shaped" portion of the Fermi surface. This seems to demonstrate that the local regions, rather than the general shape of the orbit, are responsible for the pattern of magnetoacoustic oscillations.

For the {111} face, Fig. 3 group *a*, the plotted points lie along the solid line representing the outline of the free-electron model and, therefore, clearly match a caliper dimension between centrally opposite edges of the blocked-shaped regions of the surface. As on the {110} face such regions are not strictly extremal according to the theoretical models but conceivably may contribute oscillations by virtue of a strong local coupling with the acoustic wave. The lines marked vertical locus in Fig. 3, which are centrally symmetric extremal regions and might thus be expected to contribute oscillations, evidently do not fit the data; nor apparently does the dimension between one edge of the block-shaped region and an opposite rounded knife-edge region which lies in nearly the same plane perpendicular to **q** for which conditions appear to be similar to oscillation groups *b* and *d* in Fig. 1 [{110} face]. Although fewer extrema are observed than on the {110} and {100} faces and the data is consequently somewhat less reliable, there is no obvious evidence of mixed oscillations having comparable periods. Thus, the identification of these oscillations is not entirely clear because the symmetry conditions which are required for the appearance of magnetoacoustic oscillations are not clearly apparent to us.

On the {100} face the oscillations of Fig. 4 group *b* cover the full 45° symmetry angle. As explained previously, their dimension in the [110] direction matches that observed on other faces in the same direction and thus measures the width of the "block-shaped" region. Near 0° the data points lie well within the sharp corners of the free-electron model but, as shown in Table I, are

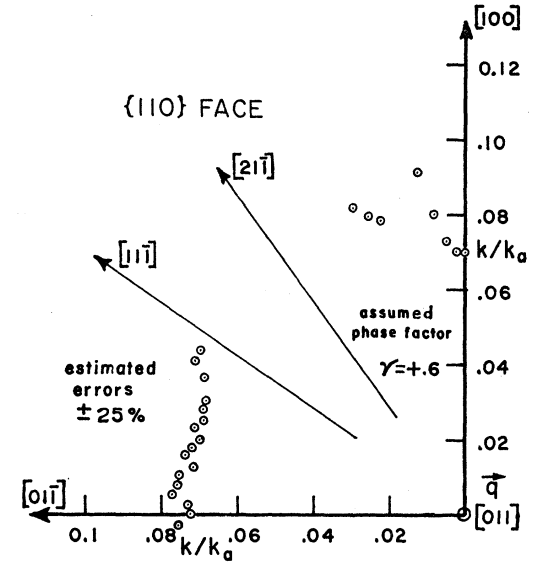

(a)

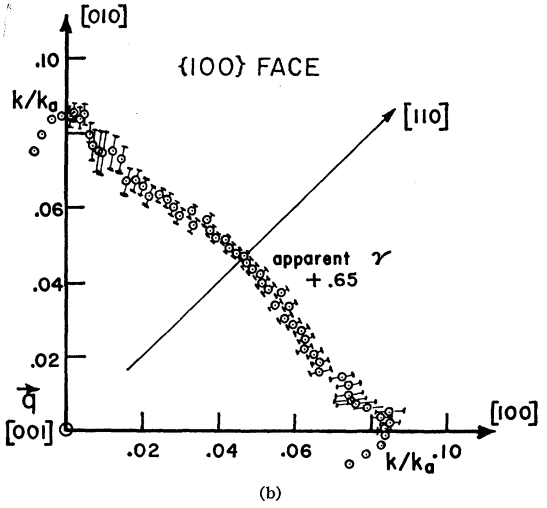

(b)

FIG. 5. Data from oscillations observed at fields between 800 and 200 Oe on the {110} and {100} faces. **q** lies perpendicular to the page, and the magnetic field is perpendicular to **q**.

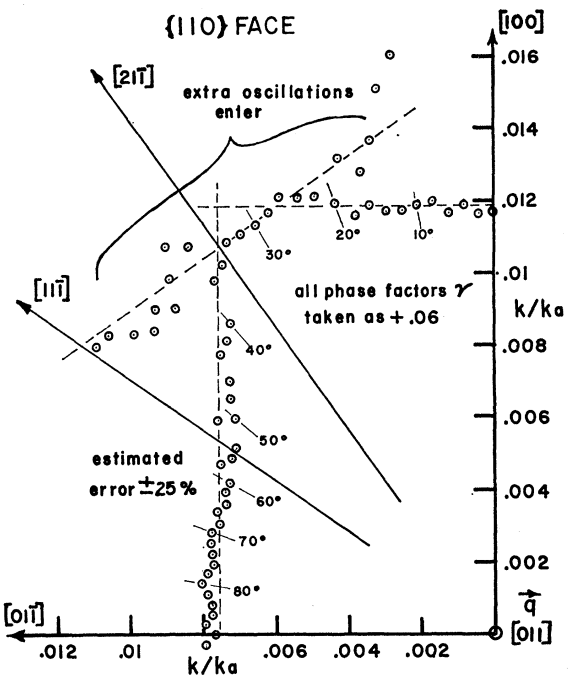

FIG. 6. The smallest measured dimensions, from oscillations observed on the {110} face at magnetic fields $H \leq 200$ Oe. **q** lies in the 011]] direction, and the magnetic field **H** lies in a (011) plane.

TABLE I. Comparison of experimental and theoretical Fermi surface dimensions—in units of k/k_a.[a,f]

Angle from [100]	Dimension interpolated from measurements	Total estimated error (%)	Free-electron dimension[b]	Calculations of Segall[c]	% Difference between measurements and Segall's calculations
{110} Face—orbits attributed to the second zone					
Fig. 1 group *a*—central orbits					
0°	0.88_5	±1.5	0.87_4	0.87_4	+1.25
5°	0.89_1	±1.5	0.88_0	0.88_0	+1.25
10°	0.91_5	±1.5	0.89_8	0.89_8	+1.9
15°	0.94_0	±2.5	0.93_0	0.92_5	+1.6
20°	0.88_0	±3.5	0.87_8	0.84_0	+4.5
25°	0.79_0	+4.0	0.77_2	0.76_0	+4.0
30°	0.73_0	±2.5	0.70_5	0.70_5	+3.5
35°	0.68_0	±2.0	0.66_4	0.66_4	+2.3
40°	0.65_0	±2.5	0.63_5	0.63_5	+2.3
45°	0.63_0	±4.0	0.61_8	0.61_8	+1.9
Fig. 1 group *d*—off-center orbits					
52.5°	0.70_7	±2.0	0.74_5	0.69_1	+2.3
55°	0.69_5	±2.5	0.72_8	0.67_7	+2.6
60°	0.67_7	±2.0	0.70_4	0.66_5	+1.8
65°	0.67_7	±2.5	0.69_5	0.66_1	+2.4
{100} Face—orbits attributed to the second zone					
Fig. 4 group *a*—compared as central orbits					
0°	0.87_8	±2.5	0.87_4	0.87_4	+0.5
5°	0.86_0	±3.5	0.88_0	0.88_0	−2.0
Fig. 1. group *b*—off-center orbits					
70°	0.33_0	±4.0	...	...	
75°	0.31_2	±2.5	...	...	
80°	0.30_0	±2.0	...	...	
85°	0.29_3	±2.0	...	...	
90°[d]	0.29_0	±2.0	...	...	
{100} Face—orbits attributed to the second zone					
Fig. 4 group *b*—central orbits					
0°	0.40_5	±2.5	0.42_0 (corners of second zone)	−3.5	
			0.41_4 (diagonal of third-zone arms)	−2.2	
5°	0.39_2	±3.5	...	...	
10°	0.36_2	±2.0	...	...	
15°	0.34_2	±2.0	...	...	
20°	0.33_0	±2.5	...	...	
25°	0.31_7	±1.5	...	...	
30°	0.31_0	±2.0	...	...	
35°	0.30_5	±2.0	...	...	
40°	0.30_0	±2.0	...	...	
45°[d]	0.30_0	±1.5	...	...	
{111} Face—orbits attributed to the second zone, measured in the ⟨110⟩ direction					
...[d]	0.29_4	±5.5	...	...	
Fig. 4 group *c*—off-center orbits, origin unknown					
45°	0.59_5	±3.0	...	...	
{110} Face—orbits attributed to third zone arms					
Fig. 5(a)—maximum diameters of arms (Δk)					
0°	0.14_0	±25	0.13_0	+7.7	
90°	0.15_0	±25	0.14_0	+6.7	
Fig. 6—minimum diameters of arms (Δk)					
0°	0.023_5	±25	0.02_7	−13	
90°	0.01_5	±25	0.05_4	...[e]	
{100} Face—orbits attributed to third zone arms					
Fig. 5(b)—maximum diameters of arms (Δk)					
0°	0.16_8	±3.0	0.18_6	−11	
20°	0.13_4	±3.5	0.15_2	−12	
30°	0.13_4	±3.0	0.14_6	−8	
40°	0.13_2	±3.0	0.14_1	−6	
45°	0.13_2	±3.0	0.14_0	−6	

[a] The dimension k_a is measured from the center of the Brillouin zone to the first zone face in the [100] direction.
[b] This assumes a sphere with volume equivalent to 3.0 electrons per atom.
[c] These dimensions assuming a Fermi energy of 0.945 Ry are taken from plots kindly supplied by Dr. B. Segall (private communication) and are based on work reported in reference 22.
[d] These dimensions measure the width of the block-shaped regions of the second zone surface. The comparable dimension between edges on the free-electron model is 0.287.
[e] These are not comparable dimensions—see text.
[f] *Note added in proof.* Recent more refined calculations by Segall reduce the differences between his theoretical results and our measurements listed in Table I (Fig. 1 groups *a* and *d*). The maximum difference is now 3.5% at 30°.

in good agreement with the calculated model of Segall. At angles within ±2° of the ⟨100⟩ directions the measured dimensions also fit the diagonal of an orbit around the inside of the third zone square arms.

At low fields the variety of oscillations observed represent values of k too small to be interpreted as orbits in the second zone. It is possible to correlate these oscillations with third zone dimensions. In Figs. 5(a) and 5(b) are plotted the data which are associated with the maximum dimensions of the third zone arms on the {110} and {100} faces, respectively, the latter being the more accurate measurements. The comparison with the calculated dimensions is shown in Table I for angles on the {100} face. The dimension in the 45° direction (the width of an arm) fits very well, and the curvature of the data points matches the curvature required by Segall's model. One would expect beats to be seen in the oscillation patterns on each side of the ⟨100⟩ directions, but these are not observed with the limited number of extrema present. On the {110} face the equivalent oscillations are generally very weak; the larger amplitudes observed near the [100] and [01$\bar{1}$] directions may arise from orbits which pass around the arms in their longer directions. The positive values of γ are consistent with an assignment of these oscillations to regions of convex curvature.

The oscillations plotted in Fig. 6 give the smallest observed values of k. If interpreted according to the calculated model of Segall, they represent the smallest cross sections of the third zone arm structure and provide evidence that these arms are not pinched off. The data points appear to lie along three lines perpendicular

to the ⟨100⟩, the ⟨110⟩, and the ⟨112⟩ directions and by their symmetry suggest small cylinders. As shown in Table I, the measured dimension in the [100] direction matches the smallest arm cross section of the calculated model. Near the [01$\bar{1}$] direction, because of the presence of the other arms, the oscillations must have a different origin. Although the measurements are poor, the dimension in the [01$\bar{1}$] direction is smaller than the arm dimensions on the calculated model, and conceivably may be associated with small regions surrounding lines of contact between the second and third zones. The oscillations on the {100} face which might be expected to make possible the assignment of these dimensions to definite regions were unfortunately not distinct enough to be analyzed.

A question arises whether the oscillations on the {100} face plotted in Fig. 4 as group *a* are to be interpreted like those of Fig. 1 group *a* as central orbits. The dimension in the ⟨100⟩ direction checks very well with that on the {110} face in the same direction, but whereas on the {110} face the oscillations are strong and are observed over a wide angle, on the {100} face they are seen only over an angular range of $\pm 5°$ and even then only at high fields. This, together with the limited angular range of groups *b* in Figs. 1 and 3 and the relative weakness of oscillations from the central orbits Fig. 1 group *a* on the {110} face in the range 16° to 20°, which might be expected to be stronger because the orbits pass over the edge regions, suggests some restriction on orbits which pass over three-sided corner regions of the second zone. Thus, we speculate that some mechanism, perhaps a direct connection, magnetic breakdown, or a scattering process, may influence orbits passing through these regions and might further make possible some extended orbits between zones.

DISCUSSION

It is a feature of the magnetoacoustic method that the same experiment can provide information on both the smallest and the largest regions of the Fermi surface. Our magnetoacoustic data taken alone are not sufficient to determine the connectivity of the second and third zones, because, like the magnetoresistance data, alternative interpretations are possible. Earlier analysis of our data[15] had led us to believe that Heine's model of a multiply connected second zone provided a good basis for interpretation of our data. However, the recent de Haas–van Alphen measurements of Gordon and Larson,[4] together with Segall's detailed model[22] of which we learned later, showed the suggestion of first zone pockets of holes to be untenable. It is still possible to interpret the smallest Fermi surface regions as direct bridges between second zones though this now seems less likely.

As noted, not all oscillations are adequately explained or uniquely identified, and the behavior of orbits which pass near the corners of the second zone appear to be anomalous. The agreement of the measured dimension with the calculated model of Segall is generally within the experimental error. The actual differences, which for concave surfaces are positive and for convex surfaces are generally negative, may be due to inaccurately assigned phase-factor values, presumably because extrema having low n numbers were, of necessity, used in much of the evaluation. For example, if a constant phase factor $\gamma=-\frac{3}{8}$ were assumed for the oscillations of Fig. 1 group *a* and a phase factor $\gamma=+\frac{3}{8}$ for those of Fig. 5(b) the differences noted in Table I between the measured values and the calculated values of Segall would be greatly reduced.

ESTIMATE OF THE RELAXATION TIME AND MEAN FREE PATH FROM MAGNETOACOUSTIC OSCILLATIONS

An estimate may be made of the electron relaxation time τ. The line of argument given here is based on that suggested by us previously for the noble metals.[31]

We begin by applying the criterion that $\omega_c\tau\approx 1$ for the last observable oscillation (with decreasing field) of a particular experimental run, where ω_c is the cyclotron frequency. The identification of the last observable oscillation is experimentally rather well defined; thus, this criterion is based on a pragmatic condition rather than a theoretical one. For the central orbit on the second zone Fermi surface observed with sound waves along [011] and magnetic field along [01$\bar{1}$] (Fig. 1 group *a*), the last observable oscillation is at a magnetic field of 500 Oe. We assume an effective mass ratio $m^*/m=0.82$, the ratio of the perimeter of this central orbit to the circumference of the equivalent circular orbit in the free-electron model; then, the relaxation time for this sample is given by $\tau=m^*c(eH_{\min})^{-1}=0.93\times 10^{-10}$ sec. The same orbit is observed on the {100} face with sound along the [001] direction and the field along the [1$\bar{1}$0] direction (Fig. 4 group *b*). For this second observation made on a different sample, the last observable oscillation occurs at 320 Oe and the corresponding relaxation time is $\tau=1.45\times 10^{-10}$ sec. If the velocity is assumed to have the free electron value, $v_0=2.03\times 10^8$ cm/sec, the corresponding mean free paths are of the order of 1.9×10^{-2} cm for the {110} sample and 3×10^{-2} cm for the {100} sample. The values of ql for a sound wave frequency of 350 Mc/sec are about 63 and 100, respectively. The resistivity ratio of the samples were not measured by us; however, the ingot from which the {100} sample was cut had, when grown, a resistivity ratio of about 8200.[25] [From the ratio of magnetic fields for the last observable oscillations, one therefore obtains a resistivity ratio of about 5250 for the {110} sample.] Cyclotron resonance effects are not to be expected at the sound frequency employed because for these samples the values of $\omega_s\tau$ is at most $\frac{1}{3}$.

REMEASUREMENT OF THE LOW-TEMPERATURE ELASTIC MODULI OF ALUMINUM

An attempt to interpret the magnetoacoustic data on the basis of the low-temperature elastic moduli for aluminum as given by Sutton[33] gave values of k which differed at all angles from a free-electron model by an amount more than could be accounted for by experimental and systematic errors, and more than seemed probable for a real metal. When all possible sources of error were examined carefully, it appeared that the values of the elastic moduli used were probably incorrect.

Several single crystal specimens were prepared, some from 99.999% pure aluminum grown by the Bridgman technique and some from material of 99.9999% purity grown by the Czochralski technique. These were cut to thicknesses of about $\frac{1}{2}$ in., respectively, aligned parallel to the {100}, {110}, and {111} crystal planes within 1° by x-ray back reflection techniques, and finally lapped flat and parallel in the manner of the magnetoacoustic specimens. An ultrasonic pulse-echo technique was used as described elsewhere.[34,35] The measurements were made at a frequency of 10 Mc/sec using both shear and longitudinal quartz plate transducers. As there was no difference in the measured velocities between the crystals grown by the Bridgman or the Czochralski techniques, most measurements were made on the latter group. Velocities were measured at room temperature, liquid-nitrogen temperature, and liquid-helium temperature and compared for internal consistency. The measured values for the adiabatic elastic moduli at room temperature are in excellent agreement with those of Schmunk and Smith[36] who used a similar experimental technique; however, they differ significantly at all measured temperatures from the values of Sutton. His low-temperature tabulated moduli were determined from measurements of the vibrational modes in small rods at temperatures from 773 to 63°K and extrapolated by him to 0°K. In Tables II and III are listed our measured values of the adiabatic elastic moduli and the longitudinal velocities in the principal crystal crystallographic directions, together with values listed by Sutton or determined from his values. In relating velocities to elastic moduli, a value of $\rho = 2.733$ g cm^{-3} for the density (obtained from the 4.2°K lattice constant value) is used. The error in the velocities is estimated to be less than $\frac{1}{2}$%. A more complete report of the elastic moduli and velocity measurements will be submitted for publication elsewhere.

TABLE II. Experimental values of the adiabatic elastic moduli in units of 10^{11} dyn cm^{-2} as determined from pulse-echo velocity measurements at 10 Mc/sec and at 4.2°K, compared with values listed by Sutton for 0°K. The estimated error is less than 1%.

Modulus	This measurement (pulse echo)	Sutton (resonant bar)	Difference in percent
c_{11}	11.438	12.30	+7.5
c_{12}	6.199	7.08	+14
$c_{11}-c_{12}$	5.238	5.22	−0.3
c_{44}	3.161	3.090	−2.2

TABLE III. Longitudinal sound velocities in the three principal crystallographic directions in units of 10^5 cm sec^{-1}, compared with values calculated from moduli listed by Sutton. The estimated error is less than $\frac{1}{2}$%.

Direction	This measurement	From moduli of Sutton	Difference in percent
⟨100⟩	6.469	6.707	+3.7
⟨110⟩	6.615	6.837	+3.3
⟨111⟩	6.670	6.880	+3.2

ACKNOWLEDGMENTS

We wish to thank Dr. B. W. Roberts of the General Electric Research Laboratory for the loan of the aluminum crystal used in the {100} face experiments, and for his friendly interest in the work. We are particularly grateful to Dr. G. A. Alers for his collaboration in the measurements of elastic moduli, which were made with his apparatus at the Ford Motor Company Scientific Laboratory. Dr. W. L. Gordon and K. Larson of the Case Institute of Technology kindly made available to us, prior to publication, their recent de Haas–van Alphen measurements on aluminum. Dr. B. Segall of the General Electric Research Laboratory generously gave us results of his Fermi surface calculations prior to publication. Dr. A. A. Galkin, Dr. V. P. Naberezhnykh, and Dr. V. L. Melnik of the Physico-Technical Institute, Academy of Sciences, Ukrainian S.S.R. were kind enough to send us a preprint of their cyclotron resonance work. It is a pleasure to acknowledge several lively discussions with Dr. R. Balcombe (Dalhousie University), Dr. M. G. Priestley (University of Chicago), Dr. T. Eck (Case Institute of Technology), Dr. A. Brailsford (Ford Scientific Laboratory), and Dr. W. A. Harrison (General Electric Research Laboratory). One of us (HVB) is indebted to Dr. A. B. Pippard and Dr. D. Shoenberg of the University of Cambridge for their valuable comments and hospitality.

[33] P. M. Sutton, Phys. Rev. **91**, 816 (1953).
[34] G. A. Alers and J. R. Neighbors, J. Phys. Chem. Solids **7**, 58 (1958).
[35] R. L. Forgas, Proc. Natl. Electron Conf. **14**, 1 (1958).
[36] R. E. Schmunk and C. S. Smith, J. Phys. Chem. Solids **9**, 100 (1959).